New ANN Method for Multi-terminal HVDC Protection Relaying

Qingqing Yang, Simon Le Blond, Raj Aggarwal, Jianwei Li

Department of Electronic and Electrical Engineering, University of Bath, United Kingdom

Abstract: This paper proposes a comprehensive novel multi-terminal HVDC protection scheme based on artificial neural network (ANN) and high frequency components detected from fault current signals only. The method is shown to accurately detect, classify and locate overhead line faults. Unlike existing traveling wave based methods which must capture the initial wavefront and require high sampling rates, the new approach is more robust since it gives accurate fault detection and fault location over a range of windowed post-fault signals. Furthermore, the proposed method is fault resistance independent meaning even a very high fault impedance has no effect on accurate fault location. A three-terminal VSC-HVDC system is modelled in PSCAD/EMTDC, which is used for obtaining the fault current data for transmission line terminals. The method is verified by studying different cases with a range of fault resistances in various fault locations, and in addition, external faults. The results show that the proposed method gives fast (<5 ms) and reliable (100%) fault detection and classification and accurate location (<1.16%) for DC line faults.

Keywords: Artificial neural network, fault current signal, fault detection, fault location, transmission line, VSC-HVDC system.

1. Introduction

Multi-terminal High Voltage Direct Current (MTDC) has often been proposed as the most promising technology for an inter-continental super-grid or collecting bulk offshore renewable energy sources [1-3]. Much renewable generation is available at locations remote from load centres, and thus must to be transported efficiently over long distances [4]. For example, to interconnect extensive offshore wind sites between Northern Europe and the UK, an offshore super-grid may be required in the future. Similarly an MTDC grid could transmit extensive solar power from the deserts of Northern Africa to the load centres of Europe.

Recent developments in DC circuit breakers and voltage source converters (VSC) make MTDC a more technically and economically feasible technology [5]. However, there are many technical challenges in evolving from point-to-point HVDC to MTDC, especially in protection systems. In typical HVDC point-to-point links, the most common method of isolation is using an AC circuit breaker to trip the entire HVDC system. Hence, the circuit breakers reside on the AC side, and in the event of a fault, the entire link is de-energised [6]. In the multi-terminal case, however, it is more desirable to isolate only the faulted link rather than trip the entire DC grid. DC circuit breakers, presently in the early stages of development, are required to isolate the faulted line. DC breakers require appropriate protective relaying, so the faults may be detected and isolated immediately. In addition, the overall protection system may require online adjustment of zonal relay settings, the faulted line may require maintenance, and the system will need restorative action, all necessitating an accurate and fast fault-location algorithm [3].

Traveling wave based protection has been successfully applied in both AC and HVDC systems by virtue of development of fast A/D conversion and numeric relay technology [7, 8]. The most common method of traveling wave based protection in multi-terminal systems, as introduced in [3, 9], is detecting the initial wavefront which has a demonstrably fast and accurate response. Due to its fast computational time and straightforward implementation, the discrete wavelet transform (DWT) is preferred for detecting arrival of wavefronts [10] over using pure frequency or time domain based methods [11]. However, limitations exist with traveling wave protection [8, 12, 13], such as lack of mathematical tools to model the traveling wave, difficulty in the detection of the wave-head, being easily influenced by noise, inability to detect close-up faults, unequal traveling wave velocities in line and underground cables, and requiring knowledge of the surge impedance and a high sampling rate.

K. De Kerf et al. proposed a DC fault detection algorithm for multi-terminal VSC-HVDC systems using three independent fault criteria, including voltage wavelet analysis, current wavelet analysis and voltage derivative and magnitude [14]. Even though the detection time reaches 1 ms, the method is only proved for a fault resistance of 0.01 Ω. In practice the fault impedance will vary, and the method presented in this new work is shown to be robust to this variation. A non-unit protection is proposed by same authors [15] based on the reflection of

the traveling wave at an inductive termination, which uses both voltage and current signals compared with a pre-selected threshold. However this method requires accurate and fast current and voltage sensors, leading to higher overall system costs than a method that relies on current signals only, such as that presented in this paper. Boundary protection is a transient-based protection concept which has been proposed in [13]. In a DC system, smoothing reactors and the capacitors installed at both ends of the DC transmission line and the inherent bus bar capacitance represent a natural boundary that does not transmit high frequency signals, and thus can be used to rapidly distinguish between internal and external faults [8]. Another transient harmonic current protection method, based on the boundary characteristic is introduced in [16]. However, this kind of transient based protection may mal-operate because of non-fault transients caused by lightning. A low speed protection for mechanical DC breakers is proposed in [17], where the total fault clearing time is in total 60 ms, a prohibitively long relaying time for most DC breakers. The backup protection proposed in the paper requires fault current limiting equipment resulting in additional costs. In [18] a data based primary fault detection method using current signals is proposed. However the fault detection relies on information from several buses in the system, and thus necessitates a fast communication link, unlike the method presented here, which uses single ended measurements for fault detection and classification. The hybrid protection presented in [8] can distinguish both non-fault lightning transients and detect close-up faults, which may be missed by traveling wave methods. However, high sampling frequencies are required, which demand more expensive hardware for sampling and calculation. Another method [12] is based on the relation between parameters of the DC transmission line and the variation of transient energy obtained from the voltage and current measurements at both terminals, although the technique is not validated with a frequency dependent line model. The authors in [16] present a method utilizing transient harmonic current based on the boundary characteristic of DC transmission lines. However, it takes a maximum of 30 ms to identify faults, which is not quick enough for protection purposes. In addition, the sensitivity of the method will decrease with increasing fault resistance. A differential protection technique for MTDC transmission lines has been proposed in [19], which depends on analysis of the high frequency transients in current signals at each line terminal. As with any differential scheme,

this relies on communication between both terminals representing a single point of failure and introducing inherent latency.

The time for the protection system to respond to a fault is particularly critical for MTDC. The present generation of DC circuit breakers need to operate within a few ms [20] (approximately 5 ms according to a manufacturer) [21, 22] to successfully interrupt the rapidly increasing DC fault current. This is technically challenging but the main fault detection proposed in this paper is always shown to robustly operate under 5 ms. With ongoing improvements in breaker technology the authors believe this will be sufficiently fast either for the current generation of breakers or in the very near future.

Artificial Intelligence (AI) is a powerful collection of computing concepts modelled on the thought and behaviour of human beings and animals. Many AI techniques attempt to automate rational decisions that would usually be made by a human expert, by including missing data, adapting to evolving situations and improving performance over long time horizons based on accumulated experience. Researchers have shown that ANNs can successfully be applied to a wide array of applications, for example reservoir inflow forecasting in hydrology [23-25]. As indicated in [26, 27], ANN based methods are effective for fault detection and fault location on AC grids and HVDC systems due to accuracy, robustness and speed. The ANN is often fed by a feature selection stage, such as the Wavelet Transform (WT). Combined sequentially, these perform fault detection, classification or location [28-30]. However, to the authors' best knowledge, there is no published work for ANNs applied to MTDC transmission protection systems.

As proposed in [31], the frequency spectrum of voltage and current contains useful information for protection purposes. The authors in [32] indicate that much of the frequency spectrum combined with an artificial neural network may be used for fault detection and fault location. Hence, the higher frequency components are selected and fed to suitably designed ANNs in this work. This paper presents a comprehensive ANN-based transient protection scheme that accurately and quickly detects, classifies and locates faults on MTDC overhead lines. The scheme is shown to have improved performance over previously used protection techniques, such as robustness to high impedance and close-up faults and excellent discrimination of external faults.

This comprehensive protection scheme based on ANNs overcomes the drawbacks of previous work, and for the first time, successfully uses wide-band information from the frequency domain for HVDC protection, opening new research avenues. The proposed method uses a larger section of the signal for detection and thus reduces the uncertainty inherent in existing travelling wave methods that rely on detection of the intial wavefront. With ANNs, the computational time is far improved, not only for fault detection, but also for fault location. The accuracy of fault detection is shown to be 100% within 4.5 ms, and location accurate to 1.16% within 25 ms compared with 1.5 s in [33] and up to 36 s in [34].

2. Multi-terminal HVDC System Modelling

A three-terminal VSC based HVDC system was modelled using the PSCAD software, based on the CIGRE B4 DC grid test system [35]. A portion of the CIGRE B4 DC grid test system, shown in Fig.1, consists of three symmetrical monopole converters, DC link capacitors, passive filters, phase reactors, transformers, DC transmission lines and AC sources.

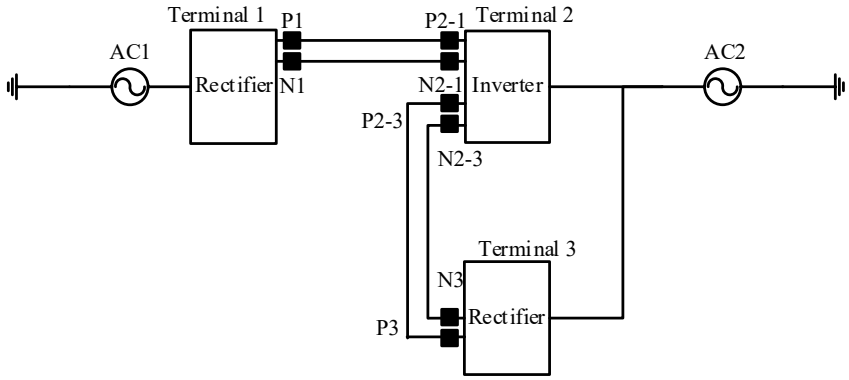

Fig. 1. The configuration of three-terminal HVDC system

2.1 Converter Station Modelling

In contrast to line-commutated, so-called current source converter (CSC) HVDC systems, VSC HVDC systems function as an ideal DC voltage source so the DC voltage polarity can remain constant when the power flow is reversed for a single VSC converter station. These capabilities make the VSC-HVDC suitable for constructing multi-terminal HVDC systems. In the simplest converter architecture, the AC voltage waveform is synthesized using a two-

level approach. The converter can be modelled as a controllable voltage source which connects to an AC network through a series reactor at the point of common coupling (PCC) [36, 37]. The basic configuration of the converter station, as well as the configuration of VSC converters of three-phase, two-level, and six-pulse bridges are presented in Fig. 2.

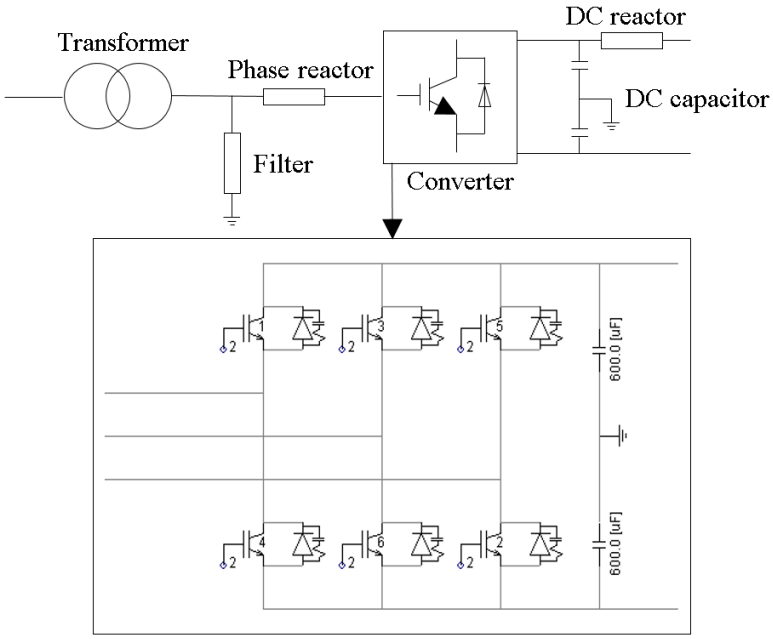

Fig. 2. Configuration of VSC converter station

Although more modern multi-level converter architectures exist, the system chosen here is the well-proven two level converter for its simplicity. On the AC side, phase reactors are applied between transformers and converters for limiting both the active and the reactive power flow by regulating currents through them. The phase reactors also function as AC filters to reduce the AC current harmonic content caused by pulse width modulated (PWM) switching of the converter station. In the well-established two-level converter stations, a low-pass LC-filter is included on the AC side which will suppress high frequency harmonic components. Capacitors on the DC side provide energy storage reducing the DC voltage ripple [38]. In addition, DC reactors are connected after DC capacitors to reduce the rate of rise of DC fault current and mitigate harmonic currents.

155 *2.2 Transmission line Model*

156 Since the transmission line is in reality made up of distributed parameters that are
157 frequency dependent, this scheme has been developed with such a line model to accurately
158 capture the high frequency transient response. The branches are exclusively overhead lines,
159 where each line is 200 km long with the geometric conductor layout illustrated in Fig.3. Each
160 line is a symmetrically grounded monopole.

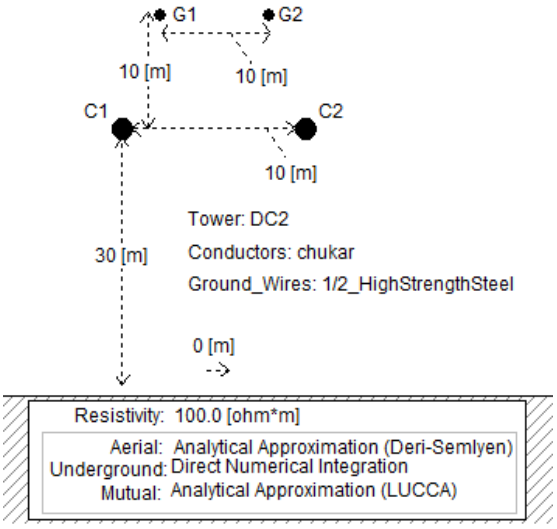

161

162 Fig. 3. The configuration of overhead transmission line model

163 For analysis of steady state conditions, the transmission line can be modelled using lumped
164 parameters, however, distributed parameters should be used to accurately reflect transient
165 behaviour [39]. The transmission line or cable can be represented by series impedances and
166 shunt admittances per unit length. The series impedance is inherently frequency dependant
167 due to its imaginary reactance and also due to the skin effect in the conductor and earth wires.
168 Based on these parameters, the characteristic parameters of the line, the surge impedance and
169 propagation constant can be derived, which determine the propagation behaviour of traveling
170 waves on the line [40].

171 *2.3 Controller Model*

172 Since this scheme relies on electromagnetic transients, it is important to model the
173 converter stations in appropriate detail, including their control systems. The coordinated

control of MTDC systems is technically challenging because the power flow and voltage must be carefully controlled at each bus by the switching of the converters. There are various competing methods of achieving this in the literature [37, 41-44]. In this paper, voltage droop control, based on system droop characteristics as discussed in [44], was chosen for the system control. This was chosen for relative simplicity and robustness since voltage droop control allows multiple converters to regulate the voltage at the same time [42]. Hence, if the control system in one terminal is disconnected, the other terminals can still regulate the voltage levels in the DC system.

The phase voltage, including the amplitude, the angle and the angular frequency can be actuated by the VSC control system. With respect to the AC or DC grid, each VSC station can be controlled in a number of different ways. Due to the decoupled current control, the active and reactive power can be dispatched independently since the two orthogonal dq-current components can be changed independently. In the modelled network shown in Fig. 1, terminal 2 is set as a slack bus to balance the system by supplying active power. Such an approach does not require communication between the terminals, because two terminals are responsible for DC voltage regulation and the remaining terminals are responsible for providing active power under both steady state and transient conditions.

To generate the reference values in the abc frame, dq control is used. The outer controller sets the droop and applies power and DC voltage limits, as shown in Fig. 4 and in equation (1).

$$\left(V_{dcref} - V_{dc}\right)K - \frac{2}{3V_d}\left(P_{ref} - P\right) = 0 \quad (1)$$

Where: V_{dcref} is the reference DC voltage, K is the proportional gain, V_d is the reference AC voltage in the dq0 reference frame and is desired to have constant value and P_{ref} is the reference active power.

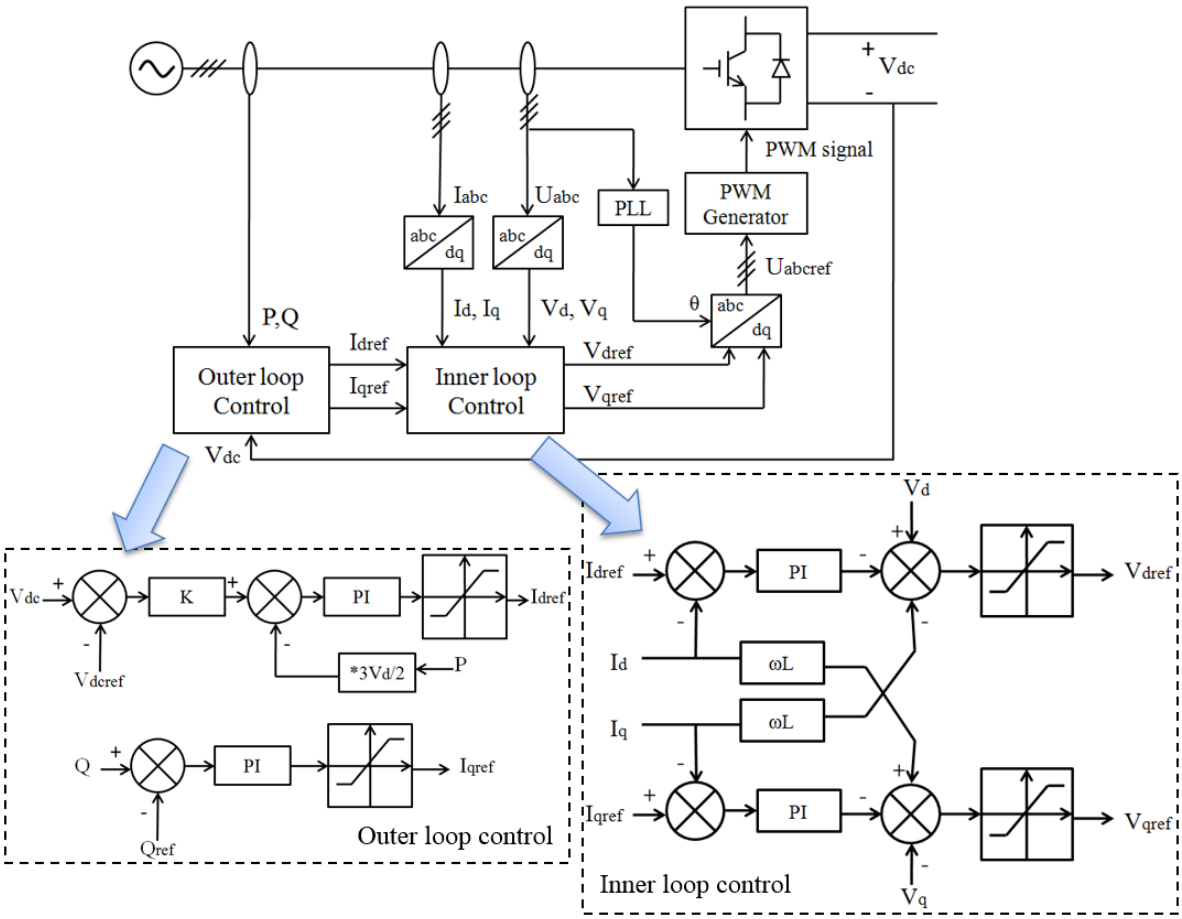

Fig. 4. The outer controller and inner controller

Using appropriately tuned PI controllers, the outer controller calculates the reference currents, I_{dref} and I_{qref}, which are the inputs to the inner control. Both active power control, P, and dc voltage control, V_{dc}, are achieved by controlling the reference to the active current controller. The I_{dref} signal is obtained by combining these two types of controllers. The reactive power, Q, controls the reactive current, I_{qref}, via a PI block as shown in Fig. 4. The droop is set by equation (2) which determines the proportional gain, K.

$$K = \frac{2P_{rated}}{3\delta_{dc}V_dV_{dcrated}} \tag{2}$$

Where: δ_{dc} is the voltage droop, P_{rated} is the rated active power, $V_{dcrated}$ is the rated DC voltage.

From a *systems* perspective, the DC bus voltage and current droop relation is directly linked to the voltage dynamics in the DC system. The current and voltage are transformed into the rotating direct-quadrature frame and the signals are passed to the inner-current PI controllers (shown in Fig. 4) that must be carefully tuned for stability. In the inner-current loop, control limits the current to protect the valves. PWM directly controls the inverter circuit switches, producing a series of pulses which have equal amplitude in the output but varying duration. The gate pulses from the PWM give the valve specific configurations to synthesise the AC waveform. Controlling the PWM can vary both the magnitude and frequency of the output voltage of the converter circuit [45].

2.4 System Transient Response

Because of their widespread distribution over an array of complex terrains and their exposure to the environment, transmission lines experience the highest occurrence of faults of any part of the power system, and therefore correct operation of their protection systems is crucial.

The most common overhead line short circuit faults, namely pole-to-pole faults and pole-to-ground faults are analysed in the simulated network. After the occurrence of a fault, low frequency steady state components and high frequency transient components due to traveling waves will be generated on the transmission line.

On the system depicted in Fig. 1, an example pole-to-pole fault on section 1 between terminal 1 and terminal 2 is applied to show the transient response of the system. The fault is at 30% of the line length from terminal 1 with 0.01 Ω fault resistance. Fig. 5 depicts the DC currents and voltages on different terminals clearly have a far more significant response to the fault on the faulted line compared to the healthy line.

The control scheme must respond quickly to preserve system stability after the faulted section is de-energised, and this necessitates detailed modelling of the control to faithfully reproduce the system's transient response. Due to PWM switching action in VSC-HVDC, the current flowing to the DC side of a converter contains harmonics, which will result in a ripple on the DC side voltage. During disturbances in the AC system (i.e. faults and switching

actions) large power oscillations may occur between the AC and the DC side. This in turn will lead to oscillations in the DC voltage and DC overvoltage that may stress the valves. The DC side capacitor (shown in Fig. 2) can mitigate this problem by providing faster converter response and energy storage to be able to control the power flow. The relatively small time constant allows fast control of active and reactive power.

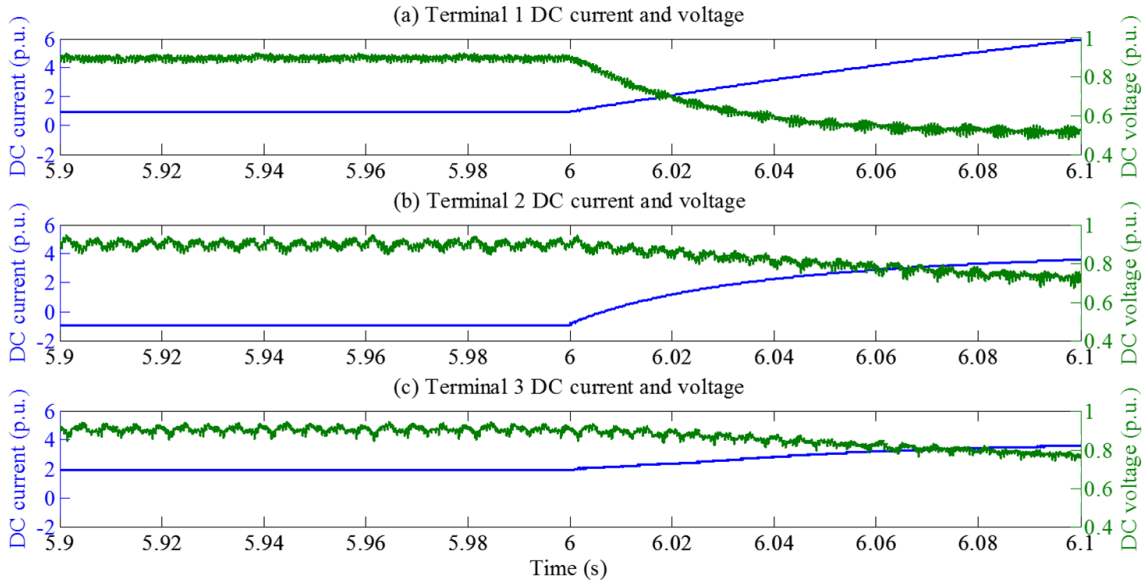

Fig. 5. The configuration of overhead transmission line

3. Signal Chain

3.1 Overview of signal chain

An overview of the signal chain is presented in Fig. 6, for fault detection and fault classification, and Fig. 7 for fault location. Firstly, a time series is generated by the digitally sampled current transducer signal. A fast Fourier transform (FFT) is applied on the windowed signal to create the input data for the ANN. A counter is then applied to the ANN to generate the diagnostic signal. Each stage is discussed in detail in forthcoming sub-sections.

3.2 Signal Processing

With the high frequency component method, the detected characteristic frequency will not propagate onto the adjacent line due to the DC shunt capacitors in the current path. Therefore

even though the DC current and voltage will be influenced during a fault on the other line, the characteristic frequency will only exist on the faulted line.

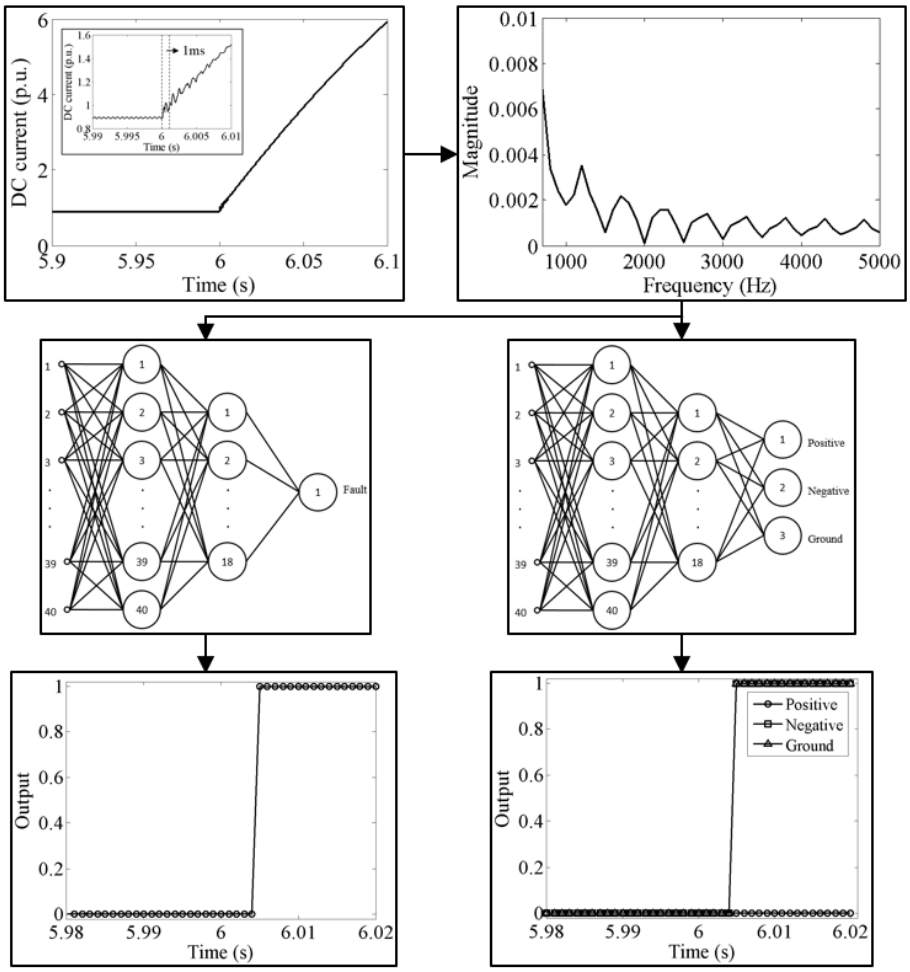

Fig. 6. Signal chain for fault detection and classification

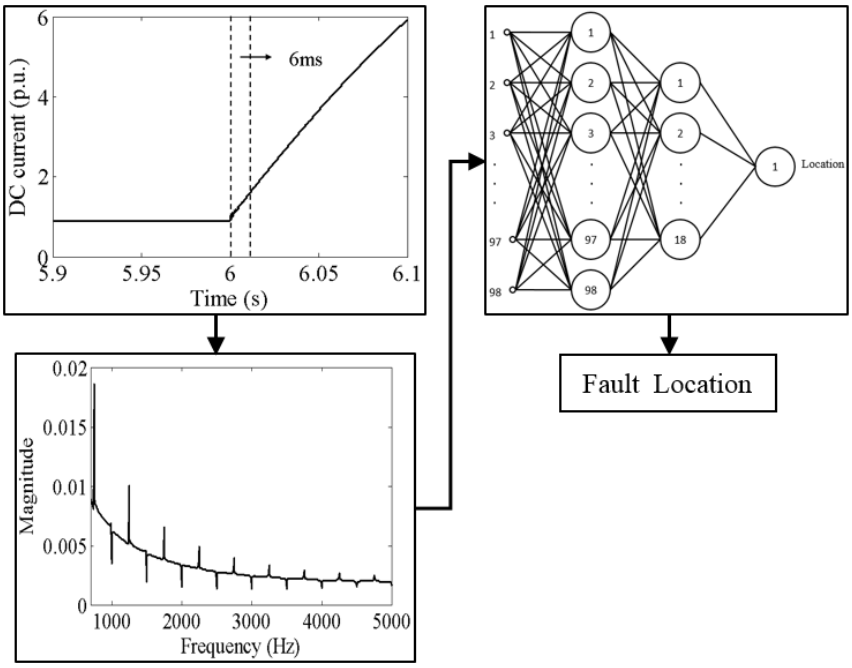

Fig. 7. Signal chain for fault location

The windowed discrete Fourier transform (DFT), implemented using the computationally efficient FFT algorithm, is a well-established method for isolating frequency components of a signal, and thus used in a variety of real time control and protection applications [46]. Extensive studies have shown that an adequate representation of frequency domain information can be obtained by an FFT with a very short window length [47]. This leaves more computational time for the rest of the relaying scheme so that the DC circuit breakers can operate within the overall protection time budget.

Following the windowed FFT on signal $f(t)$, the complex amplitude is represented by $F(\omega)$ which gives the signal's spectral components. The real parts of $F(\omega)$ are then used to indicate the magnitude at different frequencies in the windowed signal to produce a frequency spectrum. The phase information from the imaginary part of the FFT is discarded.

The technical computing environment MATLAB was used for signal processing and neural network design. The sampling frequency of 10 kHz, which translates to 200 samples per 50 Hz AC cycle, was found to be a sufficient compromise between fault location accuracy and to provide enough time for the overall relaying speed of the scheme.

The frequency spectrum generated from signal processing is shown in Fig. 8. Here, the current signal detected at terminal 1 in the system depicted in Fig. 1, is shown for the positive pole when a ground to pole fault under various conditions is simulated. The signal is windowed from the start of the fault and the window length is 6 ms. Fig. 8 (a) to (e) clearly show that only spectral features change with fault location whereas the magnitude of the spectrum changes with fault resistance. In particular, the position of the features, namely valleys and peaks, do not change with varying fault resistance, only the background level of the frequency spectrum. In contrast, the position of the features *do* vary with the location of the fault. Therefore these peaks are an important input feature to the fault location ANN.

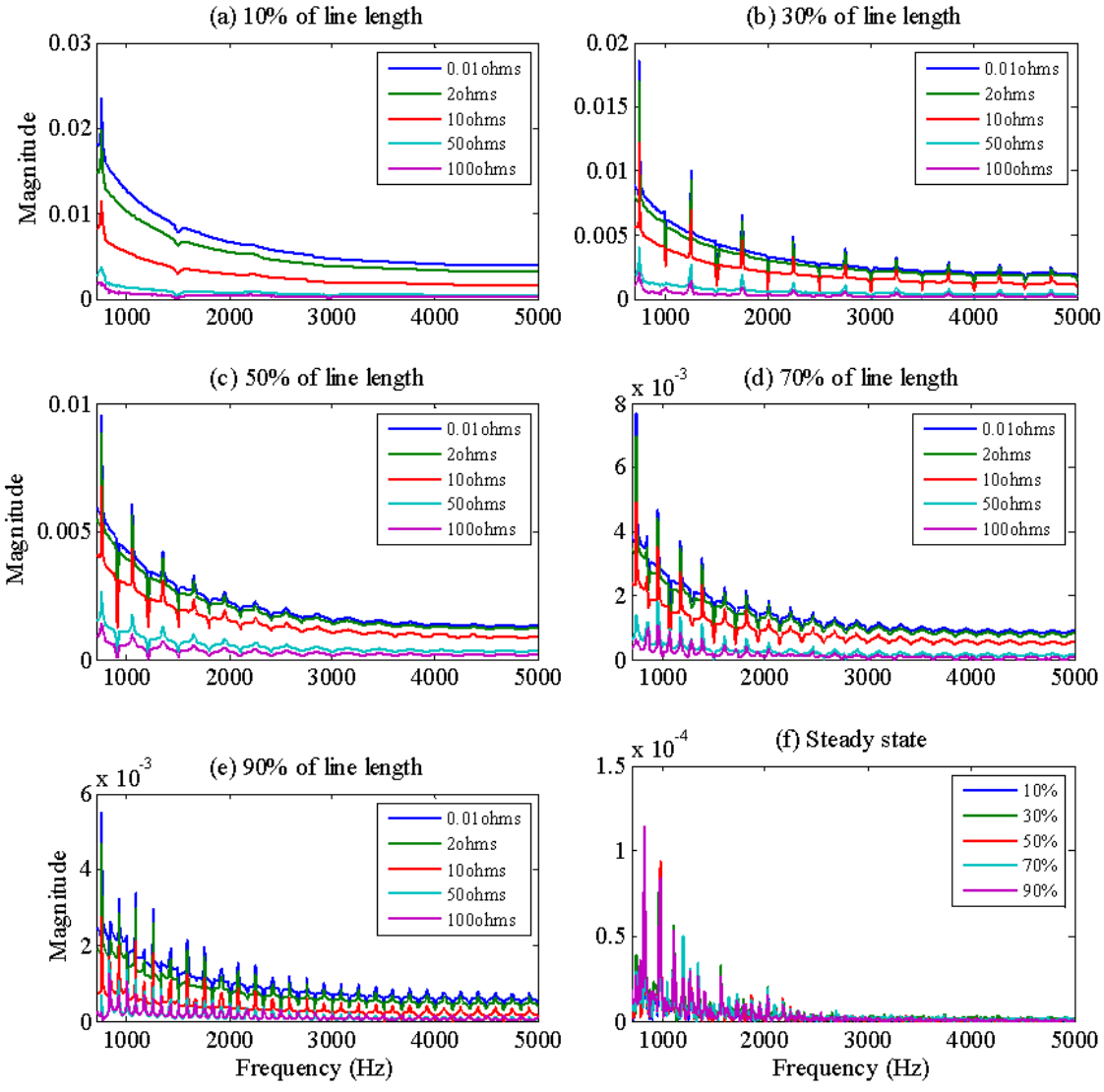

Fig. 8. Frequency spectra for different fault locations from the terminal 1, varied from 10% (a) to 90% (e) and steady state condition (f).

The high frequency components shown in Fig.8 occur because of the traveling waves that emanate from the fault location due to the sudden step change in circuit conditions. The arrival time of successive traveling waves, both original and reflected, is determined by the fault location and therefore the fault location has a direct relationship with the position of features in the frequency spectrum. The post fault frequency spectrum is largely time-independent. This increases the robustness of this frequency domain approach because regardless of the window's location on the post fault time series, it will yield a very similar frequency spectrum for some time after the fault.

Fig. 8 (f) shows the frequency spectra generated in steady state conditions for comparison. The features arise largely due to the switching of the converter stations but the magnitude of these features and the overall spectral energy under steady state conditions is negligible compared with the fault conditions.

3.3 Artificial Neural Network

Numerous ANN-based applications have been shown to give improved performance in power system protection for tasks like fault location and phase selection. This is because of the ANN's ability to discern classes in complex problem spaces, such as between transients caused by faults and those under healthy conditions [48]. To develop formal relaying schemes, precise mathematical models of each system fault condition must be constructed. However, compared with conventional formal approaches, ANNs can be trained to recognise non-linear relationships between input and output data without requiring knowledge of their internal processes. As such, using its innate ability to recognise patterns, generalise and interpolate within the parameter space, the ANN only requires simulated training data rather than extensive formal and deterministic fault and system models [49]. Importantly, after training, ANN operation time is extremely fast because it only consists of a number of simple, interconnected processing units [49].

The Fourier transform extracts a feature vector from the current waveform and feeds it to a purposefully pre-designed neural network. Since the frequency spectrum contains sufficient

information about the fault, only current signals from one terminal are required for fault detection and classification. As mentioned earlier, the frequency spectra captured for each fault case express unique features at each fault location. However due to the complexity of the mapping between spectral features and fault information, a trained ANN is an integral part of the relaying scheme. Firstly one neural network performs fault detection, namely whether the feature vector belongs to a healthy or fault condition. If a fault condition is detected, two further ANNs are trained to perform classification and fault location tasks respectively. In all cases the ANNs are multi-Layer perceptron (MLP) architectures, with the specific arrangements for each ANN shown Figs. 6 and 7 with the hyperbolic tangent sigmoid transfer function used in the hidden layers.

A window of length 1 ms is applied to capture DC current signals for fault detection and classification, whilst a 6 ms window is used for fault location. After comprehensive analysis these window lengths were empirically determined to give the best compromise between speed and accuracy for each task. Inputs are taken from standard DC current transducers and frequencies over 700 Hz of the current waveform are utilized. In the proposed fault detector and classifier, 20 frequency bands from each signal in the range 2800 Hz to 4700 Hz, each approximately 95 Hz in width, show the best performance used as ANN input. (Thus, in total, each ANN has an input layer of 40 neurons of DC current, 20 from the positive line and 20 from the negative line). The fault detection and fault classification ANN receives the same input vector with 40 inputs but they work independently from each other. For the fault location ANN, the faulty line current from both ends of the line are required with 6 ms window length. Thus in total, fault location uses 98 frequency bands between 3600 Hz and 4400 Hz, approximately 16 Hz in width, from two terminals (49 input bands from each terminal). The hidden layer consists of 18 neurons. The training data was split into 70% training samples, 15% validation samples and another 15% testing samples. For fault detection, the number of epochs was 247, for fault classification, 279, and for fault location, 189.

In order to train all three ANNs, a full range of fault scenarios were considered. Varying fault types, location, and fault resistance, for many simulation runs produced a comprehensive training set. In addition, the full range of possible healthy operational

conditions of the MTDC system, including steady state conditions, external faults, such as external DC line fault condition were simulated. Using the simulation of the system in Fig.1 and with the variables shown in Table 1, a total of 73 fault scenarios were considered, (55 DC line fault cases and 18 external fault cases). Of the fault scenarios, the training contained 10 healthy signal windows and 20 post fault input windows. In the healthy scenarios the training contained 30 consecutive windows. Hence, since each window yielded an input vector, training was completed on 2190 input vectors.

TABLE I Variables

Variable	Details
Fault location	1%, 10%, 20%, 30%, 40%, 50%, 60%, 70%, 80%, 90%, 99%
Fault resistance	0.01 Ω, 2 Ω, 10 Ω, 50 Ω, 100 Ω
External fault	AC side fault at terminal 1, 2 and 3 (single phase, double phase and three phase)

The input vectors were normalised between 0 and 1 using the maximum and minimum values encountered in the training data for each frequency band, such that 1 is the maximum and 0 is the minimum. The ANN was trained using backpropagation to produce an output vector of 1 or 0 depending on the type of fault, where '0' represents a heathy signal and '1' represents the fault signal. The transitionary case where the window captures part healthy and part faulted conditions was not used because of the ambiguity this presents in how the neural network should be trained.

At the end of the signal chain, a counter, which prevents false trips on account of noise or transitionary conditions, is applied for fault detection and classification to give a stable response. Specifically a trip signal 1 is generated after 10 consecutive ANN outputs higher than the threshold of 0.72. The counter is reset if the output falls below the threshold.

4. Test Results

Using the proposed method illustrated in the flowchart shown in Fig. 6 and Fig. 7, the fault detection, classification and location results are shown in Table 2. The accuracy of the fault location method has been evaluated with (3) to calculate the relative error:

$$e = \left|\frac{D_{act} - D_{det}}{L}\right| \quad (3)$$

Where: D_{act} is actual fault location from the measuring terminal, D_{det} is the detected fault location and L is the total length of the transmission line.

TABLE II Fault Location Result

Case	Internal /External	Section	Fault type	Fault resistance Ω	Fault detection	Positive	Negative	Ground	Fault location	Measured location	Relative error	Detection time (ms)	Classification time (ms)	Location time (ms)
1	In	S1	PG	0.25	1	1	0	1	35%	35.27%	0.27%	3.6	4.5	15.4
2	In	S1	PG	9	1	1	0	1	67%	65.98%	1.02%	3.7	4.7	20.5
3	In	S1	NG	69	1	0	1	1	89%	88.65%	0.35%	3.0	4.6	23.5
4	In	S1	NG	17	1	0	1	1	12%	12.87%	0.87%	3.9	4.8	23.6
5	In	S1	PN	32	1	1	1	0	34%	34.12%	1.12%	4.5	4.9	23.8
6	In	S1	PN	1.9	1	1	1	0	53%	52.77%	0.23%	4.1	4.9	20.4
7	In	S2	PG	0.33	1	1	0	1	78%	77.96%	0.04%	3.9	4.7	17.5
8	In	S2	PG	0.7	1	1	0	1	58%	58.47%	0.47%	3.6	4.8	17.8
9	In	S2	NG	8	1	0	1	1	24%	22.84%	1.16%	4.3	4.9	19.5
10	In	S2	NG	0.3	1	0	1	1	46%	45.68%	0.32%	3.9	4.9	21.5
11	In	S2	PN	1.2	1	1	1	0	59%	58.79%	0.21%	4.2	4.7	23.4
12	In	S2	PN	6	1	1	1	0	72%	71.13%	0.87%	4.1	4.5	25.8
13	Ex	T1	ABC	0.6	0	NA	NA	NA	NA	NA	NA	3.9	NA	NA
14	Ex	T2	AG	1.6	0	NA	NA	NA	NA	NA	NA	4.1	NA	NA
15	Ex	T3	BC	1.2	0	NA	NA	NA	NA	NA	NA	4.2	NA	NA

The protection system was tested with cases not used in the training data, with 15 separate locations and different fault types, such as positive pole to ground (PG), negative pole to ground (NG) and pole to pole (PN). The fault resistance was randomly varied within the

limits of the training parameters but values used in training were avoided. The results show that the proposed method can accurately detect, classify and locate these faults with the largest location relative error, calculated by equation (3), being less than 1.16% which is comparable to distance protection. In addition the results show that the algorithm performs successfully for a range of fault resistances. As can be seen in Table 2, with the increase in fault resistance, the percentage of error does not increase, hence, the method is not adversely affected by changing fault resistance. The maximum time for fault detection is within 4.5 ms, acceptable for DC breaker operation. The fault can be located within 26 ms which is acceptable for the automated post-fault reconfiguration of wider system settings. To achieve a fast fault location in this scheme, the error is 1%, but if a longer fault location time is permitted, the accuracy can be improved.

The protection system must be able to discriminate external faults, occurring beyond the protected zone, which in this case is the protected DC transmission line. The fault detection algorithm was trained to recognise and ignore a number of external fault conditions: namely, with reference to table 2, DC line faults, AC side faults at terminal 1, 2 and 3, (including single phase to ground (AG), double phase (BC) and three phase faults (ABC)). Using external fault cases not used in the training data showed the fault detection to be 100% successful in avoiding false trips (see table 2).

High impedance faults are generally challenging for many protection strategies because of the attenuation of the post fault characteristics and thus their resemblance to steady state pre-fault conditions. For example, it is difficult to detect faults using an overcurrent characteristic alone due to very low fault current from high impedance faults. Although absolute fault current level is slight, the current signals in the frequency domain contain enough information to indicate fault conditions. To study the sensitivity of the method proposed in this paper, the training and testing set includes a range of simulated fault resistances from 0.01 Ω to 100 Ω. As can be seen in the frequency spectrum of the fault current signal in Fig. 8, the frequency features can still be obtained under high fault resistance conditions. Therefore despite the difficulties that high impedance faults present to many existing protection techniques, the technique presented here is robust to fault impedances up to 100 Ω. Compared with the traveling wave based fault location method using a 192 kHz sampling frequency [13], the

proposed method in this paper uses a relatively low sampling frequency of 10 kHz. It is worth noting that due to the wideband information that the scheme relies on, the method will work for different sampling rates, provided the sampling is fast enough to reproduce the frequencies required by the ANN stage. Furthermore by using the windowed FFT, ANN and counter together, the scheme is more robust to noise since several frequency spectra act together to smooth out anomalies. To test this, white noise with 50 dB SNR was added to the DC current. Frequency spectra generated before and after addition of noise had exactly the same performance response to the fault location ANN.

5. Conclusion

This paper described a comprehensive novel MTDC protection scheme based on artificial neural networks. The high frequency components from fault current signals are input to specially trained ANNs. A three-terminal VSC-based HVDC model based on CIGRE B4 programme was implemented in PSCAD/EMTDC with different types of faults simulated in the DC transmission system. The general approach is valid for any MTDC system, or indeed, HVDC link, provided the system can be first simulated to generate custom ANN training data for calibration. Fault current signals were detected on all terminals in order to create frequency spectra, giving insights into the characteristic frequency components contained within the signal. Three separate neural networks for fault detection, fault classification and fault location were designed. The fault detection can detect the internal fault for both line-to-ground faults and line-to-line faults, the faulted section of the MTDC network, and distinguish external faults from internal faults. Both detection and classification only rely on single terminal measurements and so do not require a communication link, whilst the entire scheme relies only on current signals and thus DC voltage transducers are not required. The most important achievement presented is that the fault detection and classification can meet the time requirement of DC circuit breakers, and the fault location is accurate and fast enough for online, automation of wider system protection settings if desired. The proposed method is demonstrably robust to high resistance faults and noise. Since the method is purposefully designed for multi-terminal systems, it is robust to faults on other DC lines. Although it is sufficiently fast, the fault detection is not as fast as some existing methods, but importantly

unlike the traveling-wave methods that only rely on the initial wavefront, more of the post-fault signal is used, offering the 100% reliability demonstrated in the results.

With the rapid development of HVDC technology, MMC converters are now the state of the art. However there are a wide range of competing MMC topologies available, from different manufacturers, with no one option prevailing across the few installed systems across the world. Thus for the sake of simplicity, and to demonstrate the approach on the most developed technology, the well-established 2-level converter was used to validate the presented method. In future work, this new method will be demonstrated on a wide range of MMC converter systems. However, regardless of the nature of the converter station, the authors are confident the method will be valid as long as training data is available for the ANNs via simulation.

The training process is important for the robustness of the method. Since the simulation work must prove the concept first on one system, the training data is limited to one system in this paper. In order to reduce the uncertainties, more training data will be used to produce a more generic system in later work. In order to achieve the best compromise between fault location time and the accuracy, a comparison between different window lengths will be conducted to investigate the best performance between speed and accuracy. More extensive training data from different systems will be used to generalize the ANN responses.

Acknowledgment

The authors gratefully acknowledge the support and use of facilities in the department of Electronic and Electrical Engineering, University of Bath, UK. Q. Yang would like to thank the support provided by Chinese Scholarship Council.

References

[1] S. Gordon, Supergrid to the rescue, Power Engineer, 20 (2006) 30-33.
[2] D. Van Hertem, M. Ghandhari, Multi-terminal VSC HVDC for the European supergrid: Obstacles, Renewable and sustainable energy reviews, 14 (2010) 3156-3163.
[3] S. Azizi, M. Sanaye-Pasand, M. Abedini, A. Hassani, A Traveling-Wave-Based Methodology for Wide-Area Fault Location in Multiterminal DC Systems, Power Delivery, IEEE Transactions on, 29 (2014) 2552-2560.
[4] O. Gomis-Bellmunt, J. Liang, J. Ekanayake, R. King, N. Jenkins, Topologies of multiterminal HVDC-VSC transmission for large offshore wind farms, Electric Power Systems Research, 81 (2011) 271-281.
[5] N. Flourentzou, V.G. Agelidis, G.D. Demetriades, VSC-Based HVDC Power Transmission Systems: An Overview, Power Electronics, IEEE Transactions on, 24 (2009) 592-602.
[6] K. Sano, M. Takasaki, A surgeless solid-state DC circuit breaker for voltage-source-converter-based HVDC systems, Industry Applications, IEEE Transactions on, 50 (2014) 2690-2699.

[7] V. Pathirana, P. McLaren, A hybrid algorithm for high speed transmission line protection, Power Delivery, IEEE Transactions on, 20 (2005) 2422-2428.
[8] X. Liu, A.H. Osman, O.P. Malik, Real-time implementation of a hybrid protection scheme for bipolar HVDC line using FPGA, Power Delivery, IEEE Transactions on, 26 (2011) 101-108.
[9] O. Nanayakkara, A.D. Rajapakse, R. Wachal, Traveling-wave-based line fault location in star-connected multiterminal HVDC systems, Power Delivery, IEEE Transactions on, 27 (2012) 2286-2294.
[10] O.M.K.K. Nanayakkara, A.D. Rajapakse, R. Wachal, Location of DC Line Faults in Conventional HVDC Systems With Segments of Cables and Overhead Lines Using Terminal Measurements, Power Delivery, IEEE Transactions on, 27 (2012) 279-288.
[11] M.M. Saha, J.J. Izykowski, E. Rosolowski, Fault location on power networks, Springer Science & Business Media, 2009.
[12] X. Zheng, T. Nengling, Y. Guangliang, D. Haoyin, A transient protection scheme for HVDC transmission line, Power Delivery, IEEE Transactions on, 27 (2012) 718-724.
[13] X. Liu, A. Osman, O. Malik, Hybrid traveling wave/boundary protection for monopolar HVDC line, Power Delivery, IEEE Transactions on, 24 (2009) 569-578.
[14] K. De Kerf, K. Srivastava, M. Reza, D. Bekaert, S. Cole, D. Van Hertem, R. Belmans, Wavelet-based protection strategy for DC faults in multi-terminal VSC HVDC systems, Generation, Transmission & Distribution, IET, 5 (2011) 496-503.
[15] W. Leterme, J. Beerten, D. Van Hertem, Nonunit Protection of HVDC Grids With Inductive DC Cable Termination, IEEE Transactions on Power Delivery, 31 (2016) 820-828.
[16] Z. Xiao-Dong, T. Neng-Ling, J.S. Thorp, Y. Guang-Liang, A transient harmonic current protection scheme for HVDC transmission line, Power Delivery, IEEE Transactions on, 27 (2012) 2278-2285.
[17] M. Hajian, L. Zhang, D. Jovcic, DC transmission grid with low-speed protection using mechanical DC circuit breakers, IEEE Transactions on Power Delivery, 30 (2015) 1383-1391.
[18] S.P. Azad, W. Leterme, D. Van Hertem, A DC grid primary protection algorithm based on current measurements, in: Power Electronics and Applications (EPE'15 ECCE-Europe), 2015 17th European Conference on, IEEE, 2015, pp. 1-10.
[19] A.E. Abu-Elanien, A.A. Elserougi, A.S. Abdel-Khalik, A.M. Massoud, S. Ahmed, A differential protection technique for multi-terminal HVDC, Electric Power Systems Research, 130 (2016) 78-88.
[20] O.G.-B. Dirk Van Hertem, Jun Liang, HVDC Grids: For Offshore and Supergrid of the Future, April 2016.
[21] M. Callavik, A. Blomberg, J. Häfner, B. Jacobsen, The hybrid HVDC breaker. An innovation breakthrough enabling reliable HVDC grids. ABB Grid Systems, in, 2013.
[22] ABB, ABB's Hybrid HVDC Circuit Breaker, http://new.abb.com/about/events/cigre2014/hvdc-breaker, (2014).
[23] M. Valipour, Optimization of neural networks for precipitation analysis in a humid region to detect drought and wet year alarms, Meteorological Applications, 23 (2016) 91-100.
[24] M. Valipour, M. Banihabib, S. Behbahani, Monthly inflow forecasting using autoregressive artificial neural network, Journal of Applied Sciences, 12 (2012) 2139.
[25] M. Valipour, M.E. Banihabib, S.M.R. Behbahani, Comparison of the ARMA, ARIMA, and the autoregressive artificial neural network models in forecasting the monthly inflow of Dez dam reservoir, Journal of hydrology, 476 (2013) 433-441.
[26] M. Mirzaei, M. Ab Kadir, E. Moazami, H. Hizam, Review of fault location methods for distribution power system, Australian Journal of Basic and Applied Sciences, 3 (2009) 2670-2676.
[27] N. Zhang, M. Kezunovic, Transmission line boundary protection using wavelet transform and neural network, Power Delivery, IEEE Transactions on, 22 (2007) 859-869.
[28] K. Silva, B. Souza, N. Brito, Fault detection and classification in transmission lines based on wavelet transform and ANN, Power Delivery, IEEE Transactions on, 21 (2006) 2058-2063.
[29] A.L.O. Fernandez, N.K.I. Ghonaim, A novel approach using a FIRANN for fault detection and direction estimation for high-voltage transmission lines, Power Delivery, IEEE Transactions on, 17 (2002) 894-900.
[30] F. Martín, J.A. Aguado, Wavelet-based ANN approach for transmission line protection, Power Delivery, IEEE Transactions on, 18 (2003) 1572-1574.
[31] S. Le Blond, R. Bertho, D. Coury, J. Vieira, Design of protection schemes for multi-terminal HVDC systems, Renewable and Sustainable Energy Reviews, 56 (2016) 965-974.
[32] S.P. Le Blond, Q. Deng, M. Burgin, High frequency protection scheme for multi-terminal HVDC overhead lines, in: Developments in Power System Protection (DPSP 2014), 12th IET International Conference on, 2014, pp. 1-5.
[33] J. Liu, J. Duan, H. Lu, Y. Sun, Fault Location Method Based on EEMD and Traveling-Wave Speed Characteristics for HVDC Transmission Lines, Journal of Power and Energy Engineering, 3 (2015) 106.
[34] S. Marx, B.K. Johnson, A. Guzmán, V. Skendzic, M.V. Mynam, Traveling Wave Fault Location in Protective Relays: Design, Testing, and Results, in: proceedings of the 16th Annual Georgia Tech Fault and Disturbance Analysis Conference, Atlanta, GA, 2013.
[35] T.K. Vrana, Y. Yang, D. Jovcic, S. Dennetire, J. Jardini, H. Saad, The CIGRE B4 DC grid test system, System, 500 (2013) D1.
[36] J. Beerten, S. Cole, R. Belmans, Modeling of multi-terminal VSC HVDC systems with distributed DC voltage control, Power Systems, IEEE Transactions on, 29 (2014) 34-42.
[37] R.T. Pinto, P. Bauer, S.F. Rodrigues, E.J. Wiggelinkhuizen, J. Pierik, B. Ferreira, A novel distributed direct-voltage control strategy for grid integration of offshore wind energy systems through MTDC network, Industrial Electronics, IEEE Transactions on, 60 (2013) 2429-2441.
[38] D. Jovcic, K. Ahmed, High Voltage Direct Current Transmission: Converters, Systems and DC Grids, John Wiley & Sons, 2015.
[39] C. Wadhwa, High voltage engineering, New Age International, 2007.
[40] A. Wasserrab, G. Balzer, The significance of frequency-dependent overhead lines for the calculation of HVDC line short-circuit currents, Electrical Engineering, (2015) 1-11.
[41] J. Khazaei, Z. Miao, L. Piyasinghe, L. Fan, Minimizing DC system loss in multi-terminal HVDC systems through adaptive droop control, Electric Power Systems Research, 126 (2015) 78-86.
[42] C. Dierckxsens, K. Srivastava, M. Reza, S. Cole, J. Beerten, R. Belmans, A distributed DC voltage control method for VSC MTDC systems, Electric Power Systems Research, 82 (2012) 54-58.
[43] X. Zhao, K. Li, Droop setting design for multi-terminal HVDC grids considering voltage deviation impacts, Electric Power Systems Research, 123 (2015) 67-75.
[44] T.M. Haileselassie, Control of multi-terminal VSC-HVDC systems, (2008).

[45] A. Lindberg, T. Larsson, Pwm And Control Of Three Level Voltage Source Converters In An Hvdc Back-to-back Station, in: AC and DC Power Transmission, Sixth International Conference on (Conf. Publ. No. 423), 1996, pp. 297-302.
[46] Y. Guo, M. Kezunovic, D. Chen, Simplified algorithms for removal of the effect of exponentially decaying DC-offset on the Fourier algorithm, Power Delivery, IEEE Transactions on, 18 (2003) 711-717.
[47] E.C. Ifeachor, B.W. Jervis, Digital signal processing: a practical approach, Pearson Education, 2002.
[48] Q.-H. Wu, Z. Lu, T. Ji, Protective relaying of power systems using mathematical morphology, Springer Science & Business Media, 2009.
[49] T.S. Dillon, D. Niebur, Neural networks applications in power systems, CRL Publishing London, 1996.